*J. Biochem.* 2009;146(1)23–32
doi:10.1093/jb/mvp040

# Characterization of putative tryptophan monooxygenase from *Ralstonia solanasearum*

**Nami Kurosawa[1], Tomoko Hirata[2] and Haruo Suzuki[1,2,*]**

*[1]Department of Biosciences, School of Science; and [2]Division of Biosciences, The Graduate School of Fundamental Life Science, Kitasato University, Kitasato 1-15-1, Sagamihara-shi, Kanagawa-ken 228-8555, Japan*

Received January 9, 2009; accepted February 25, 2009; published online March 20, 2009

**The amino-acid sequence of a putative tryptophan monooxygenase (PTMO) from *Ralstonia solanacearum* is homologous with that of proenzyme (proPAO) of L-Phe oxidase (deaminating and decarboxylating) (PAO) from *Pseudomonas* sp. P-501 in their overall sequences. PTMO was expressed in *E. coli* and purified, but had no catalytic activity to oxidize L-Phe. By treating PTMO with various proteases, the Pronase-treated PTMO (PTMOp) showed a relatively high activity to oxidize L-Phe, L-Trp, L-Tyr and L-Met. Studies on the stoichiometry of the reaction showed that L-Phe and L-Tyr were mostly oxygenated, that L-Met was mostly oxidized, and both oxygenation and oxidation of L-Trp was observed. Initial velocity patterns were a ping-pong type with L-Phe and L-Tyr, and a sequential type with L-Trp and L-Met as substrate. The spectrum of enzymes with sufficient amounts of these substrates to reduce the enzyme showed a long wavelength species (purple complex) with L-Phe, but not with L-Tyr, L-Trp and L-Met. These results lead to the conclusion that PTMO and PTMOp belong to proPAO and PAO, respectively.**

**Key words: flavoproteins, proteolytic activation, tryptophan monooxygenase, steady-state kinetics, stoichiometry of reaction.**

Abbreviations: IAA, indole-3-acetic acid; IPTG, isopropyl-β-D-thiogalactopyranoside; PAO, L-phenylalanine oxidase; PAOpt, PAO activated by Pronase and trypsin; proPAO, noncatalytic proenzyme of PAO; PTMO, putative tryptophan monooxygenase; PTMOp, PTMO activated by Pronase; X-gal, 5-bromo-4-chloro-3-indoltl-β-D-galactoside.

## INTRODUCTION

L-Phe oxidase (EC 1.13.12.9: PAO) from *Pseudomonas* sp. P-501 catalyses both the oxidative deamination and oxygenative decarboxylation of L-Phe, L-Tyr and L-Met as substrate (*1–3*). The enzyme was screened from bacteria in soil for the determination of L-Phe in a clinical laboratory (*4*, *5*). The enzyme contains 2 mol of noncovalent FAD (*2*) and 2 mol each of α and β subunits per mole of enzyme (*6*). Previously we reported the sequencing and expression of the L-Phe oxidase gene from *Pseudomonas* sp. P-501 (*7*). A homology search of the sequence revealed a putative L-Trp monooxygenase (PTMO) from *Ralstonia solanacearum* with 63.5% identity, but L-Trp 2-monooxygenase with low scores (*7*, *8*). This protein was the only one with the highest homology when we began this study, and it is therefore interesting to see if PTMO is the L-Phe oxidase. During the preparation of this article, we again performed a homology search of the proPAO sequence (*9*), and another protein homologous to proPAO was found in the genome sequence of *R. solanacearum* Race 3Biovar 2 (63.7% identity) (*10*). The sequence is 82.0% identical to that of PTMO (Fig. 1).

*Ralstonia solanacearum* is considered to be one of the most important plant pathogenic bacteria, infecting plants through root wounds, causing wilt, and leading to plant death [see ref. (*11*) for review and references therein]. This mode of invasion differs from that of most bacterial pathogens which cause tumours and galls in plants (*12–14*). In tumour- and gall-forming bacteria, indole-3-acetic acid (IAA) is synthesized and involved in pathogenesis. Synthesis of IAA occurs by the following reactions: L-Trp → indoleacetamide → IAA, catalysed by tryptophan 2-monooxygenase and indoleacetamide hydrolase, respectively. Various aspects of tryptophan 2-monooxygenase have been extensively studied (*15–17*). The *R. solanacearum* genome contains a putative indoleacetamide hydrolase in addition to PTMO (*8*), and the signalling molecules such as IAA and ethylene gas are likely to be implicated in the wilting process (*11*).

The present work aimed to see if a putative *R. solanacearum* tryptophan monooxygenase belongs to L-Phe oxidase (deaminating and decarboxylating), since PTMO was the only protein with a highly homologous sequence with PAO when we started the present work. This article reports the expression, purification and characterization of PTMO. The results show that PTMO is a pro-enzyme proteolytically activated with proteases, and that the Pronase-activated form (PTMOp) of PTMO catalysed both the oxidative deamination and oxygenative decarboxylation of L-Phe, L-Tyr and

*To whom correspondence should be addressed. Tel: +81-42-741-5526; E-mail: suzukih@kitasato-u.ac.jp

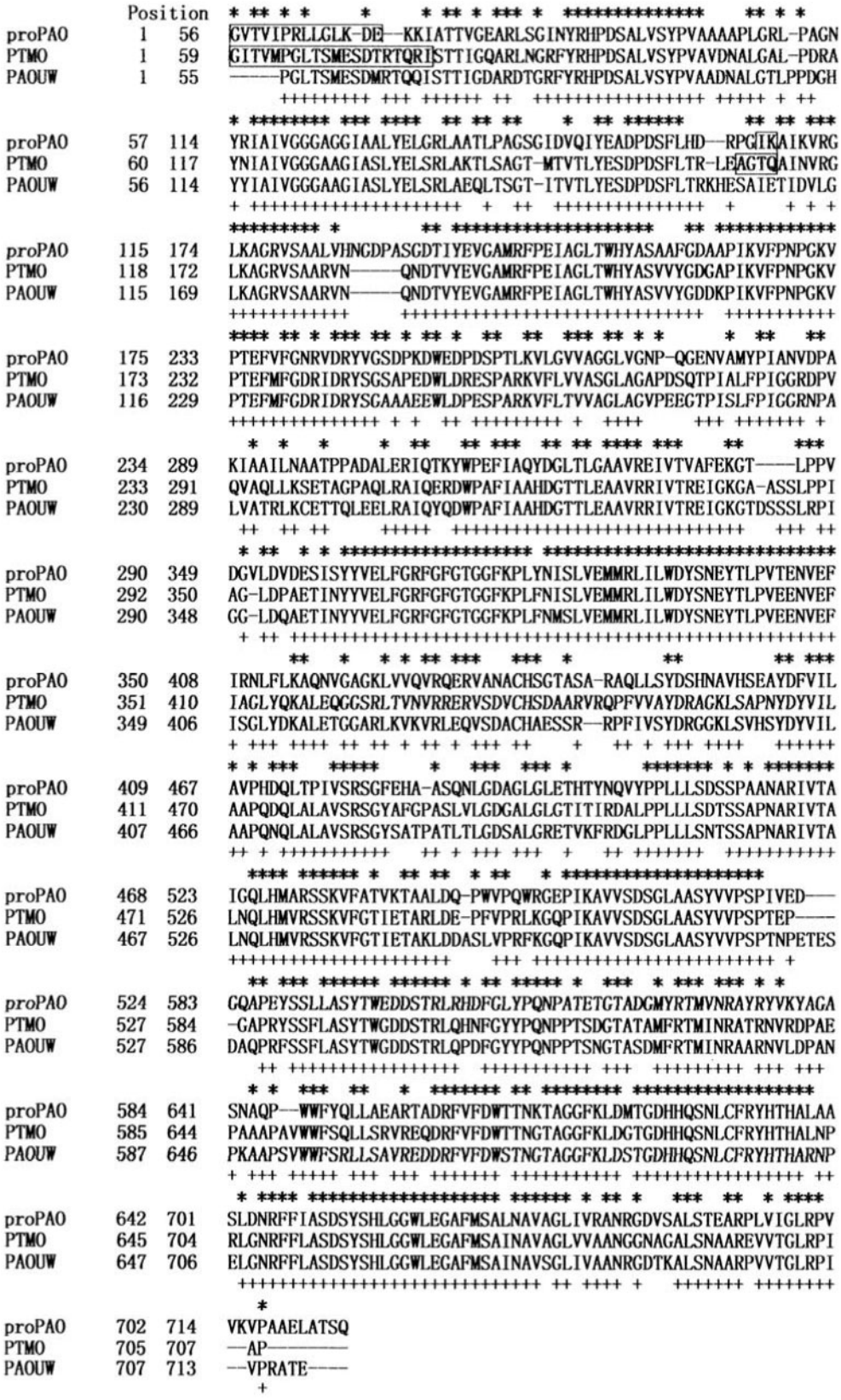


Fig. 1. **Alignment of the amino-acid sequences of proPAO, PTMO, and PAOUW.** (*) Residues conserved between proPAO and PTMO, (+) residues conserved between PTMO and PAOUW (*R. solanacearum* R3B2 UW551) (*10*).

L-Trp, and the oxidative deamination of L-Met. These properties, the structural comparison of PTMO with proPAO (*18*), and the steady-state kinetic properties of PTMOp lead us to conclude that PTMO and PTMOp belong to proPAO and PAO, respectively.

## MATERIALS AND METHODS

*Materials*—Pfu Ultra High-Fidelity DNA Polymerase was obtained from STRATAGENE. Protein markers, Broad Range and Kaleidscope, were from BIO-RAD. IPTG, X-gal and dNTP mixture were from Takara Biomedicals. DEAE-Sepharose and Ni-Sepharose 6 Fast Flow were from Amersham Pharmacia Biotech. All restriction endonucleases were from Roche. Pronase and trypsin were from Sigma and Worthington, respectively. Lysylendopeptidase and V8 protease were from Wako Chemicals. Oligonucleotide primers were obtained from Qiagen. All other chemicals used were reagent grade.

*Cells, Strains and Plasmid—E. coli* clones harbouring plasmid pBR322 was kindly supplied by Dr Christian Boucher, France (*8*). pBR322 contains the open reading frame of PTMO. pBluescript II KS (+) was from Stratagene, and pET vector 22b (+) was from Novagen. Trypton peptone and Bacto yeast extract were from Difco. Two different bacterial growth media, LB and TP (*19*), were used in the present experiments. LB: 5 g Bacto yeast extract, 10 g Bacto tryptone, and 10 g NaCl were dissolved in 1 l water. TP: 15 g Bacto yeast extract, 20 g Bacto tryptone, 8 g NaCl, 2 g $Na_2HPO_4$ and 1 g $KH_2PO_4$ were dissolved in 1 l water, and 1 ml of 0.2 g/ml glucose was added just before use (*19*). *E. coli* strains JM109 and BL21 (DE3) were from Novagen.

*Construction of Expression Vector for PTMO*—Using pBR322 as a template, a DNA fragment containing the PTMO sequence was obtained by PCR using a forward primer, 5′-GTCATATGGGTATTACCGTCAT GCCGG-3′ (the *Nde*I site is underlined), and a reverse primer, 5′-AAACTCGAGCGGCGCGATGGGCC GC-3′ (the *Xho*I site is underlined). The PCR primers were designed on the basis of the sequence of the PTMO gene (*8*). PCR products were inserted into the *Eco*RV site of pBluescript vector. Formation of a restriction enzyme site was confirmed by DNA sequencing. The plasmids were digested with *Xho*I and *Nde*I. The fragments were purified by agarose-gel electrophoresis, and inserted into the *Nde*I-*Xho*I site of pET 22b(+), and transformed into *E. coli* BL21(DE3). The expression vector obtained was named pPTMO. The sequence of the insert was confirmed by sequencing the insert. DNA sequencing was conducted by the Genomic Research Department, Shimadzu-Biotech.

*Expression of Gene Encoding PTMO, and Purification of PTMO—E. coli* BL21(DE3)/pPTMO cells were grown in 5 ml LB medium containing ampicillin (50 μg/ml) for 8 h at 37°C. The culture medium (1 ml) was added to 1 l of TP medium containing 50 μg/ml ampicillin and cultured for 16 h at 30°C. The cultured cells were collected by centrifugation at 6,000 rpm for 15 min at 4°C and washed with buffer A (20 mM Tris–HCl pH 7.9, 500 mM NaCl), suspended in buffer A, and lysed by sonication using a Branson sonicator (Model 250, 5 output, 40 duty cycles) below 7°C under constant mixing of the cell suspension. Cell debris was removed by centrifugation and the supernatant was applied to a His-Bind resin column (Ni Sepharose 6 Fast Flow) equilibrated with buffer A. PTMO was eluted from the column by a linear concentration gradient of imidazole in buffer A. The absorbance of the eluates was monitored at 280 nm, and the fraction containing PTMO was collected. The purity of PTMO was confirmed by SDS/PAGE. The protein concentration was determined by measuring the absorbance at 280 nm assuming an absorbance coefficient of $A_{1\%/1\,cm} = 19.7$ (*2*). The amount of bound-flavin was determined spectrophotometrically using an extinction coefficient of 11.3 $mM^{-1}\,cm^{-1}$ at 465 nm (*2*).

*Protein Sequence Analysis*—The amino-acid sequences of proteins and peptide fragments were analysed with a gas-phase sequencer (Shimadzu, PPSQ-10).

*Assay of Enzyme Activity*—The rate of the overall reaction was estimated by measuring the consumption of oxygen dissolved in the reaction mixture with a Clark-type oxygen electrode (Strathkelvin Instruments). The reaction mixture contained various concentrations of substrate in 20 mM potassium phosphate buffer, pH 7.0 at 25°C. The reaction was initiated by addition of the enzyme. Before measurements, the initial concentration of molecular oxygen in the reaction mixture was adjusted to the desired value by bubbling oxygen or nitrogen gas through the reaction medium. The temperature of the reaction mixture was controlled at 25°C by circulation of water at a constant temperature through a jacket around the reaction vessel. The rate of the overall reaction ($v/e_o$) is expressed as moles of oxygen consumed per second per mole of the flavin moiety of enzyme. To estimate kinetic parameters, the least-square regression method was used (*20*).

*$H_2O_2$ and $NH_3$ Measurements*—Hydrogen peroxide produced by the oxidation of substrates was measured as follows. The reaction mixture (400 μl) in a cuvette contained 1 mM substrate, 200 μl of the *o*-dianisidine solution and 4 μl peroxidase (10 mg/ml) in 20 mM Tris–HCl (pH 8.0) at 25°C. The reactions were monitored at 500 nm, and after oxygen uptake had ceased, the change of $A_{500}$ was measured to determine the amount of the oxidized dianisidine formed by using the extinction coefficient of *o*-dianisidine to be 6.36 $mM^{-1}\,cm^{-1}$ at 500 nm (*21*). The solution of *o*-dianisidine used was prepared by dissolving 10 mg of *o*-dianisidine in 1 ml ethanol, and the solution was centrifuged for 5 min at 14,000 rpm. The supernatant was collected and diluted by the addition of a 19-fold excess of deionized water (*7*).

The amount of ammonia was measured enzymatically using the L-glutamate dehydrogenase-coupled method. The reaction mixture (100 μl) contained 100 μM L-amino acid, 0.5 mM α-keto glutarate, 0.5 mM NADPH, 50 nM PTMOp and 1 μl glutamate dehydrogenase (10 μg) in 20 mM Tris–HCl (pH 8.0). At given times, the absorbance at 340 nm was measured, and the amount of ammonia formed was determined using the extinction coefficient of NADPH (6.2 $mM^{-1}\,cm^{-1}$) at 340 nm.

*Reversed-Phase High Performance Liquid Chromatography*—When L-Phe and L-Trp were used as

substrate, the amounts of products formed were determined by high performance liquid chromatography (*1*, *15*, *22*). The products analysed were phenylacetamide, phenyl pyruvic acid, indoleacetamide and indole pyruvic acid. The reaction mixture was comprised of 200 μM substrate amino acids, 50 nM PTMOp and 20 mM potassium phosphate (pH 7.0) in a total volume of 1 ml, and incubated for 15 min at 25°C, and the reaction was stopped by adding 1 ml of perchloric acid. After centrifugation of the mixture, 200 μl of the supernatant was loaded on a chromolith$^{TM}$ RP-18e ODS-Hypersil column (4.6 × 100 mm) and eluted with a linear gradient of acetonitrile containing 0.1% trifluoroacetic acid. The absorbance at 220 or 280 nm was monitored to detect the products using a Jasco LC-1500 apparatus (Jasco, Tokyo).

*Absorption Spectra*—Absorption spectra were measured in a double beam spectrophotometer, type V-520-SR or type V560, from Japan Spectroscopic.

*Structural Model-Building*—The structural model of PTMO was built by using a computer analysis available on the World Wide Web, Geno3D (PoleBio-Informatique Lyonnais, http://pbil.ibcp.fr) (*23*). Model analyses were performed with PyMOL (http://pymol.sourceforg.ne).

## RESULTS

*Expression of PTMO Gene in E. coli*—Preliminary experiments showed that the PTMO gene was expressed well as a soluble protein under the conditions similar to those used in the expression of the proPAO gene. That is, *E. coli* BL21 (DE3) cells harbouring pPTMO were cultured overnight in TP medium in the absence of IPTG at 30°C, and the cells harvested from the culture medium were used to prepare PTMO as described in MATERIALS AND METHODS section. The amount of purified PTMO was ~15 mg from 4.5 g wet weight of *E. coli* cells (1 l of TP medium). The purified PTMO showed a single band on the SDS–PAGE gel (Fig. 2) and a typical flavoprotein spectrum with maxima at 389 and 468 nm. The protein did not show activity to oxidize L-Phe, but showed activity after Pronase treatment of PTMO, as described in the following section.

*Proteolytic Activation of PTMO*—First, we tried various proteases, such as trypsin, chymotrypin, lysylendopeptidase and V8 protease to activate PTMO. After incubation of PTMO (16.7 μg) with 1.6 μg of these proteases in 1 ml of 50 mM Tris–HCl (pH 8.0) for 2.5 h at 25°C, part of the incubation mixture was assayed using L-Phe as substrate. In the proteases used, Pronase was most effective for activation. Trypsin, chymotrypsin, V8 protease and lysylendoprotease also activated PTMO, but the activity obtained using these proteases was ~5% of that with Pronase. Therefore, we treated PTMO with Pronase to prepare the active PTMO. To find the better conditions to prepare the Pronase-activated PTMO (PTMOp hereafter), PTMO (10 mg) was incubated with Pronase (1 mg) in 1 ml of 50 mM Tris–HCl (pH 8.0) at 25°C, then part of the incubation mixture was taken to assay the enzyme activity at 0.5, 1, 2, 4, 6, 8 and 24 h. The enzyme activity rose progressively to reach a plateau at 4 h and remained constant thereafter up to 24 h.

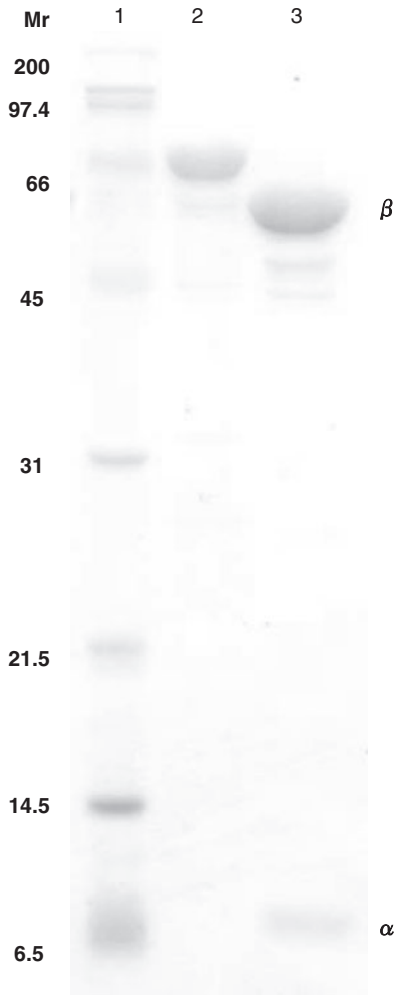


Fig. 2. **SDS/PAGE of PTMO and PTMOp.** Lane 1, PTMO. Lane 2, PTMOp. M, molecular weight maker.

Therefore, to prepare PTMOp, we usually incubated PTMO with Pronase for 3–4 h under the condition described above. PTMOp was purified by a chromatographic procedure using a Hi-Trap DEAE-FF column (Amersham Biosciences). From 10 mg of PTMO, 8.6 mg of the purified PTMOp was obtained. As Fig. 2 shows, PTMO was cleaved into two main polypeptides, α and β subunits. Gel-filtration chromatography of the purified PTMOp was performed using Superdex 200 prep grade (Amersham, 120 ml) in 20 mM Tris–HCl (pH 8.0) containing 150 mM NaCl. The protein was eluted as a single peak with Mr 162,000, suggesting that PTMOp is comprised of two moles of each subunit, $\alpha_2\beta_2$.

N-terminal sequence analysis of PTMOp suggested two sequences, AINVRGLKAGRVSA (218/241/184/209/92/160/237/196/276/169/79/235/39/240) and STTIGQARLNG (48/85/78/160/111/105/220/94/180/140/139), comparing the amount of PTH amino acids of each Edman cycle with the amino-acid sequence of PTMO (Fig. 1). In these sequences, the numbers in parentheses after each sequence are pmoles of PTH amino acids recovered in each Edman cycle starting at the N-terminal amino-acid residue. The molecular mass of PTMOp was determined

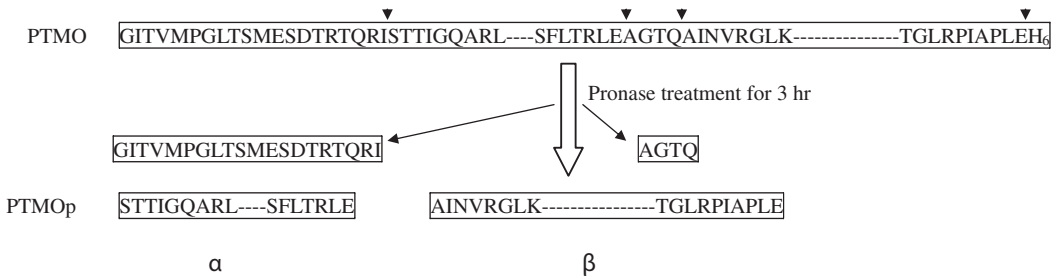


Scheme. 1.

Table 1. **Stoichiometry of the PTMOp-catalysed reaction**

| | Amino acid | Amino acid added (nmol) | $NH_3$ formed (nmol) | Oxidation (%) |
|---|---|---|---|---|
| **Exp. 1** | L-Phe | 25 | 0.63 ± 0.21 | 2.5 ± 0.9 |
| | L-Tyr | 11 | 0.85 ± 0.24 | 7.7 ± 0.22 |
| | L-Trp | 25 | 9.74 ± 0.73 | 39.0 ± 2.9 |
| | L-Met | 10 | 11.7 ± 0.21 | 117.7 ± 2.1 |
| | **Amino acid** | **Amino acid added (nmol)** | **$H_2O_2$ formed (μM)** | **Oxidation (%)[a]** |
| **Exp. 2** | L-Phe | 1.0 mM | 8.8 ± 2.3 | 3.4 ± 0.9 |
| | L-Tyr | 1.0 mM | 5.6 ± 0.3 | 2.2 ± 0.1 |
| | L-Trp | 1.0 mM | 91.2 ± 11.9 | 35.3 ± 4.6 |
| | L-Met | 1.0 mM | 267 ± 45 | 103.5 ± 17.4 |
| | **Amino acid** | **Amino acid added (nmol)** | **Phenylacetamide formed (nmol)** | **Phenylpyruvic acid formed (nmol)** |
| **Exp. 3** | L-Phe | 200 μM | 18.8 ± 0.3 (93.8 ± 1.3)[b] | 1.2 ± 0.3(6.2 ± 1.3)[c] |
| | | | **Indoleacetamide formed (nmol)** | **Indolepyruvic acid formed (nmol)** |
| | L-Trp | 200 μM | 12.5 ± 0.4 (62.7 ± 1.9)[b] | 7.5 ± 0.4 (37.3 ± 1.9)[c] |

The values were calculated from four determinations in Exp. 1, five determinations in Exp. 2 and eight determinations in Exp. 3. In Exp. 3, one-tenth of the reaction mixture was analysed. [a]Oxidation (%) was calculated by assuming that the initial concentration of oxygen in the reaction mixture was 258 μM. The amount of L-Phe or L-Trp added was 20 nmol, and the [b,c]numbers in parentheses are the percentage of oxygenation and oxidation reactions, respectively.

using the purified protein. The mass spectrum showed two major peaks with masses of 9,191.1 and 64,499.8. Combining these results with the N-terminal sequences, the sequence of the α subunit is from Ser21 to Glu107, and that of the β subunit from Ala112 to Glu708. The molecular weight of each subunit was calculated as 9,191 for the α subunit and 64,485 for the β subunit from the sequences, which agree well with the corresponding masses. These results allowed us to propose that PTMO is proteolytically activated, as shown in Scheme 1. This activation process is similar to that of proPAO. But, in the case of proPAO activation, the most effective activation was observed with Pronase-trypsin treatment with a low yield of PAOpt (less than 5%) (*7*), but PTMO was efficiently activated with high yield (80%).

*Enzymatic Properties of PTMOp*—The results described above lead to the notion that PTMOp belongs to L-Phe oxidase (EC 1.13.12.9) purified from *Pseudomonas* sp. P-501. To clarify this idea, we characterized the enzymatic properties. First, we tested the substrate specificity of the enzyme. The activity of PTMOp was determined with 20 kinds of 1 mM L-amino acids in 20 mM Tris–HCl (pH 8.0) at 25°C. The activity ($v/e_o$) was 89.5 ± 6.8, 47.3 ± 8.3, 49.5 ± 2.6 and 28.7 ± 4.4 $s^{-1}$ for L-Phe, L-Tyr, L-Trp and L-Met, respectively, and less than 5% of that of L-Phe for L-Lys, L-His and L-Thr, and the other 13 L-amino acids did not show activity. Moreover, D-Phe showed no activity. Thus, L-Phe is clearly the best substrate, followed by L-Tyr, L-Trp and L-Met.

*Stoichiometry of the Reaction Catalysed by PTMOp*—PAO catalyses both the oxidative deamination and oxygenative decarboxylation of L-Phe. Therefore, we analysed the reaction catalysed by PTMOp using L-Phe, L-Tyr, L-Trp and L-Met as substrate. The reaction was monitored by measuring the amounts of hydrogen peroxide and ammonia formed for these amino acids. As for L-Phe and L-Trp, the amounts of α-keto acids and amides formed by the enzyme reaction were determined by HPLC. Table 1 shows the results obtained. L-Phe and L-Tyr were mostly oxygenated, and L-Met was mostly oxidized. But, L-Trp was oxidized nearly 40% and oxygenated nearly 60%.

*Effect of pH on the Activity of Enzyme*—Effect of pH on enzyme activity was determined by measuring the oxygen uptake in 50 mM buffer in the presence of

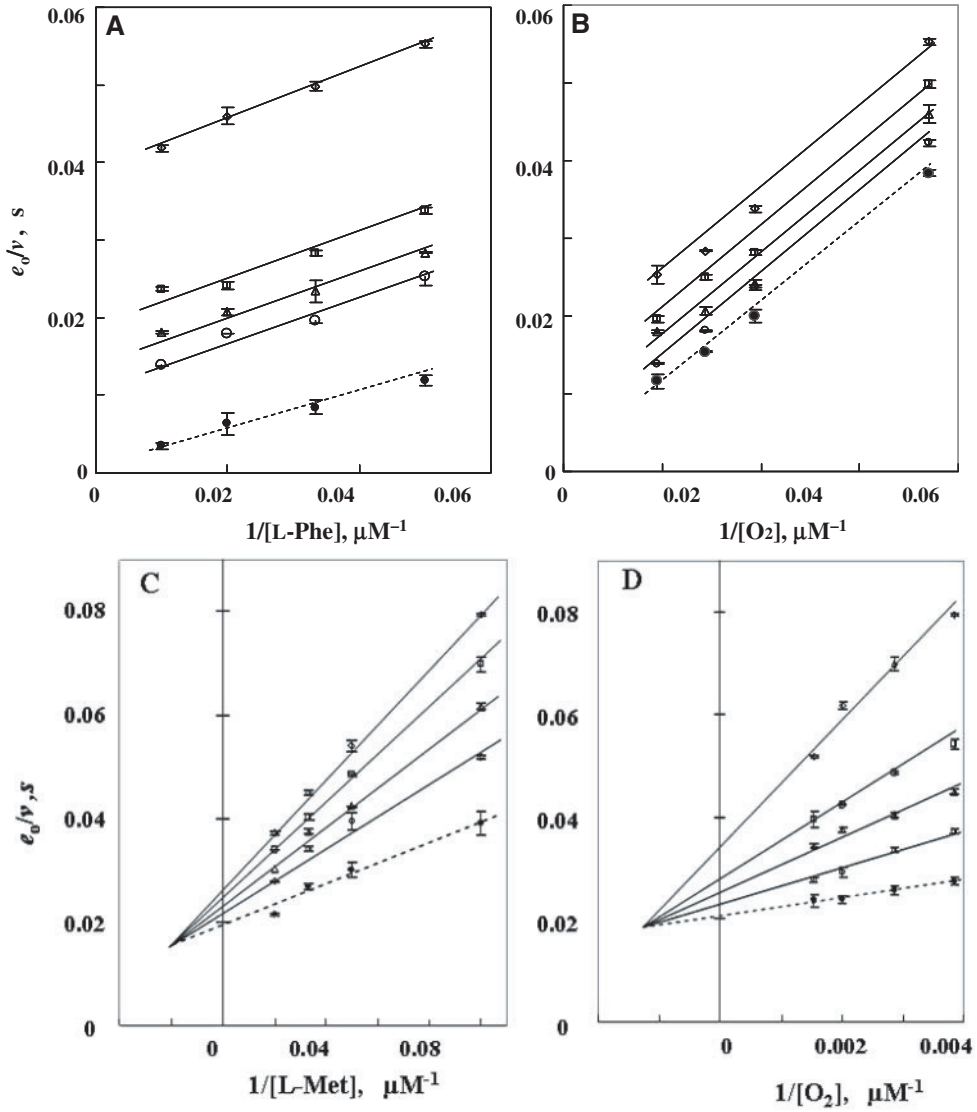


Fig. 3. **Effect of various concentrations of L-Phe, L-Met and oxygen on the reaction rate of PTMOp.** (A) Plots of $e/v$ versus 1/[L-Phe]. The oxygen concentration is 137 μM (open rhombus), 259 μM (open square), 350 μM (open triangle), 525 μM (open circle), and the infinite oxygen concentration (filled circle). The enzyme conontration is 20 nM. The reaction mixtures 20 mM potassium phosphate buffer, pH 7.0. B: plots of $e/v$ versus 1/[$O_2$]. L-Phe concentration is 20 μM (open rhombus), 30 μM (open square), 50 μM (open triangle), 100 μM (open circle) and the infinite L-Phe concentration (filled circle). C: Plots of $e_o/v$ versus 1/[L-Met]. The oxygen concentration is 262 μM (open rhombus), 353 μM (open square), 532 μM (open triangle), 635 μM (open cirlce) and the infinite oxygen concentration (filled cirlce). D: Plots of slope versus 1/[$O_2$]. L-Met concentration is 20 μM (open rhombus), 30 μM (open square), 50 μM (open triangle), 100 μM (open circle) and the infinite L-Phe concentration (filled circle).

0.2 mM L-Phe and 10 nM PTMOp at 25°C. The buffers used were sodium acetate for pH 3.5–5.5, potassium phosphate for pH 6.0–8.0, pyrophosphate for 8.0–9.5 and borate–NaOH for pH 9.5–11.0. Optimum pH was around pH 7.0, and almost the same activity was observed at pH 6.5–7.5 (data not shown). The optimum pH of PAO was reported to be wider than that of PTMOp, that is, pH 6–9 (*2*). Following the experimental conditions of PAO, some of the experiments described above were performed at pH 8.0, but the following were done mostly at pH 7.0.

*The Steady-State Kinetics*—The rate of overall reaction was determined at pH 7.0 by measuring the oxygen uptake at various concentrations of L-amino-acid substrates and oxygen. The double reciprocal plots between $e_o/v$ versus 1/[S] at various concentrations of oxygen gave a series of parallel straight lines with L-Phe (Fig. 3A). Similar results were obtained when the same set of data was replotted versus 1/[$O_2$] (Fig. 3B). Secondary plots of $Y$ intercepts from Fig. 3B (or Fig. 3A) versus 1/[L-Phe] (or 1/[$O_2$]) gave a straight line, respectively, and were used to determine values for the steady-state kinetic parameters (Table 2). Straight parallel lines were also observed for the plots of $e_o/v$ versus 1/[L-Tyr] or 1/[$O_2$] at various $O_2$ or L-Tyr concentrations, respectively (data not

Table 2. **Kinetic parameters estimated from steady-state kinetics.**

| Substrate | $V_m/e_o$ ($s^{-1}$)[a] | $K_m$ [S](μM) | $V_m/e_o$ ($s^{-1}$)[b] | $K_mO_2$ (μM) |
|---|---|---|---|---|
| L-Phe | 575 ± 290 (1,850[c]) | 118 ± 59 (100[c]) | 765 ± 272 | 3817 ± 1412 (1,840[d]) |
| L-Tyr | 255 ± 64 (3,570) | 715 ± 22 (4,000) | 344 ± 34 | 1740 ± 1960 (3,145) |
| L-Met | 53.6 ± 4.2 (286) | 112 ± 21 (2,200) | 47.9 ± 1.8 | 80.7 ± 17.7 (1,258) |
| L-Trp | 57.9 ± 9.1 | 34.3 ± 2.2 | 33.5 ± 1.5 | 38.9 ± 17.1 |

[a]Values determined from the plots of $e_o/v$ versus 1/[S] at the infinite concentration of L-amino acid. [b]Values determined from the plots of $e_o/v$ versus $1/[O_2]$ at the infinite concentration of oxygen. [c]Values in parenthesis are those reported for PAO (*24*). [d]Values in parenthesis are calculated from the data reported for PAO, though $X–O_2$ complex was not assumed (*24*).

shown). From the plots, steady-state kinetic parameters were determined (Table 2).

The data obtained with L-Met and L-Trp were different from those described for L-Phe and L-Tyr. The double reciprocal plots of $e_o/v$ versus 1/[L-Met] or $1/[O_2]$ at various $O_2$ or L-Met concentrations, respectively, gave lines intersecting at the left of the ordinate (Fig. 3C and D). Secondary plots of $Y$ intersects from Fig. 3D (or Fig. 3C) versus 1/[L-Met] (or $1/[O_2]$) gave a straight line, respectively, and were used to determine values for the steady-state kinetic parameters (Table 2). Similar data were obtained with L-Trp, and values for the steady-state kinetic parameters were similarly obtained. The parameters obtained are summarized in Table 2.

*Absorption Spectra*—L-Phe was added to the oxidized form of enzyme at a final concentration of 1 mM in 20 mM Tris–HCl buffer (pH 8.0) under aerobic conditions, and the spectrum was measured immediately after the addition of L-Phe. The spectrum of the oxidized form of enzyme changed to a typical purple complex observed with PAO, having a characteristic broad absorption band around 550 nm (Fig. 4) (*24*). This broad band decayed very slowly to the reduced level. On the other hand, when L-Tyr, L-Trp or L-Met were mixed at a final concentration of 1 mM with PTMOp, the yellow colour of enzyme disappeared before the spectral measurements. These spectral properties of PTMOp are different from those observed with PAO (*24*).

## DISCUSSION

The present work aimed to see if a putative tryptophan monooxygenase of *R. solanacearum* belongs to L-Phe oxidase (deaminating and decarboxylating), since PTMO was the only protein having a highly homologous sequence with PAO, though we noticed another protein (in *R. solanacearum* R3B2 UW551) homologous with PAO (see Fig. 1) during the preparation of this manuscript. The results described in the above section lead us to conclude that PTMO and PTMOp belong to proPAO and PAO, respectively.

*Role of PTMO in Pathogenesis*—The present results show that PTMO and PTMOp belong to proPAO and PAO, respectively. As Table 1 shows, PTMOp catalyses the formation of indoleacetamide from L-Trp, though the activity is relatively low. Therefore, the role of PTMOp is probably to produce indoleaceamide, leading to the synthesis of IAA. Unlike tumour- and gall-forming bacteria (*12–14*), which contain the active L-Trp 2-monooxygenase, *R. solanasearum* produces inactive PTMO, which is proteolytically activated to form PTMOp. It is not known if PTMO is activated in the cell of *R. solanasearum*. For the preparation of PAO, autolysis of *Pseudomonas* sp. P-501 is essential, and the addition of Pronase to the lysate increased the yield of PAO (*1*). These facts indicate that PAO is expressed as an inactive form proPAO in the bacterial cell. Therefore, it is conceivable that PTMO is activated in the host plant xylem tissue after secretion from the bacteria, and catalyses the formation of indoleacetamide, thus leading to the formation of IAA.

*Properties of PTMO*—The 3D structures of proPAO showed us the unique nature of the proteolytic activation of the enzyme (*9*). That is, the prosequence occupies the 'amino-acid channel' which leads amino-acid substrate from the outside of enzyme protein to the interior flavin site. The problem in the preparation of the activated form of PAO (PAOpt) was its low yield (less than 5%). When we stocked a solution of PAOpt with low activity for several weeks at 4°C, we noticed that PAOpt began to show enhanced activity. On the other hand, we obtained PTMOp with high yield (~80%). The difference in the nature of this pro-enzyme is likely to have derived from the difference in the interaction of prosequence with the amino-acid residues surrounding the prosequence. To clarify this point, we constructed a 3D structure of PTMO using Geno3D (*23*) and a 3D structure of proPAO as template (2YR4.pdb). As Fig. 5A shows, the overall structure of PTMO matches well with that of proPAO, especially their secondary structure and N-terminal region. In the prosequence of proPAO, the structure of G1 to R7, which occupies the amino-acid channel, merges well with that of the corresponding sequence of PTMO (Fig. 5B), and the amino-acid residues interacting with G1 to P6 are similar to each other. But the side chain of R7 in proPAO interacts with four amino-acid residues, A210, G211, G215 and N216, but G7 of PTMO does not interact with the corresponding residues, A208, S209, G213 and A214. Therefore it is highly possible that these interactions of Arg7 in proPAO continue to bind the propeptide with the channel even after proteolytic cleavage, thus inhibiting the enzyme activity, and leading to low yield of preparation of PAOpt. On the other hand, the prosequence in PTMO does not have this interaction, then the propeptide is released easily from PTMOp after proteolytic cleavage, thus PTMOp was prepared with high yield. This consideration might be tested by site-directed mutagenesis studies of R7G mutation of proPAO or G7R mutation of PTMO.

Construction of a structural model of the N-terminal region of PAOUW was not successful by Geno3D, since

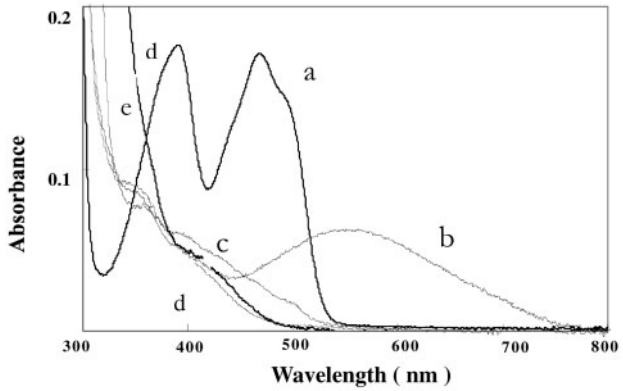


Fig. 4. **Spectral change of PTMOp with 1 mM L-amino acids in 20 mM Tris–HCl (pH 8.0).** Spectra were obtained before (A) and after addition of L-Phe (B), L-Tyr (c), L-Trp (d) and L-Met (e) at room temperature under aerobic conditions.

the N-terminal sequence of PAOUW (*10*) does not have five residues found in N-terminal sequences of proPAO and PTMO (Fig. 1). The five residues sequence occupies the amino-acid channel in the proPAO and PTMO structures; therefore, it is interesting to know whether or not the sequence (PGLTS) of PAOUW has a role occupying the channel. This will be clarified by structural and functional analyses of PAOUW.

*Catalytic Mechanism of PTMOp*—To compare the kinetic parameters of PTMOp with those of PAO, the available data for PAO are for L-Phe, L-Tyr and L-Met as substrate (Table 2). From these parameters, $(V_m/e_o)/K_m{}^S$ values are roughly estimated. The value for L-Phe of both enzymes is higher than that for L-Tyr and L-Met, and the value for L-Phe of PAO ($1.85 \times 10^7\,M^{-1}s^{-1}$) is $\sim$4 times higher than that of PTMOp ($4.9 \times 10^6\,M^{-1}\,s^{-1}$), suggesting that the catalytic efficiency to L-Phe is higher with PAO than with PTMOp.

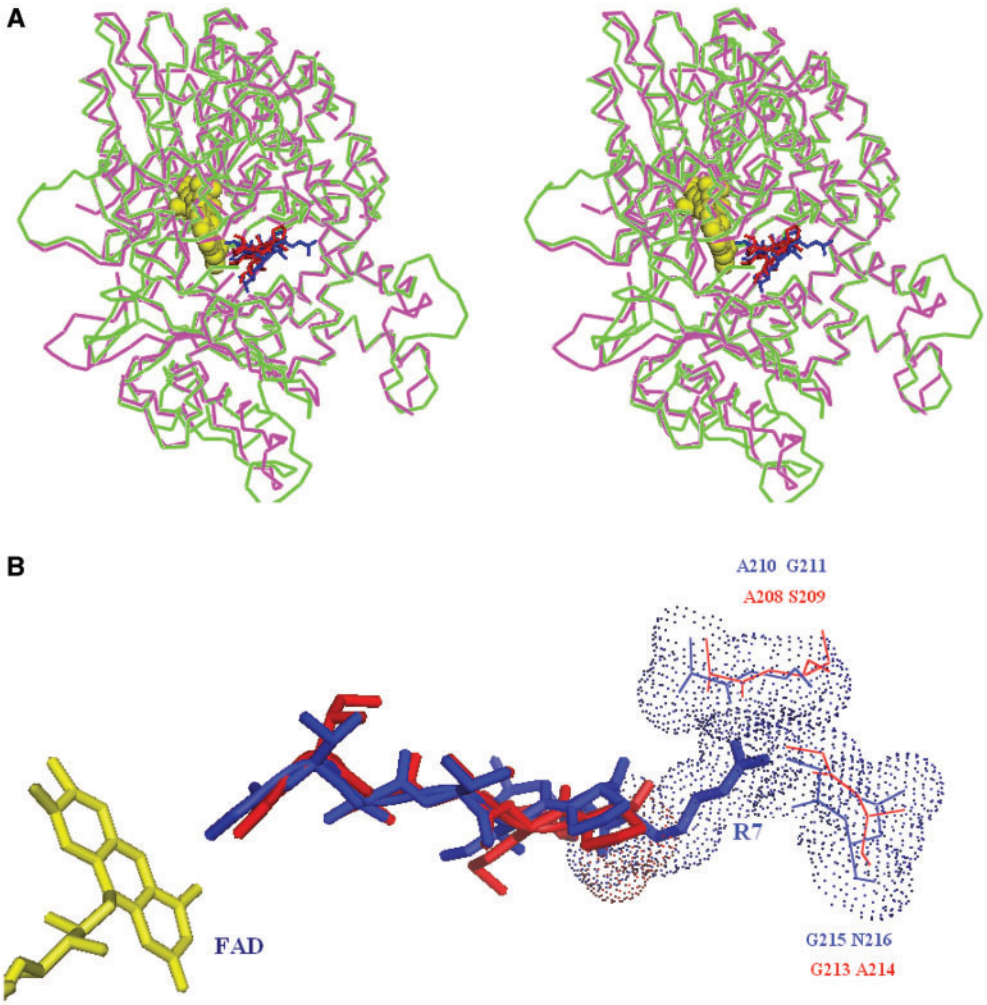


Fig. 5. **Structural model of PTMO. (A) The stereo view of the superimposition of PTMO monomer (green) and proPAO monomer (pink, 2YR4.pdb).** FAD is shown in a yellow sphere. N-terminal pro-sequences are shown as red stick (GITVMPGL, PTMO) and blue stick models (GVTVIPRL, proPAO). (B) The superimposition of pro-sequence of PTMO (red stick) and of proPAO (blue stick). The side chain of R7 (proPAO) interacts with A210, G211, G215 and N216, but G7 (PTMO) does not interact with the corresponding residues (A208, S-209, G213, A214).

The steady-state rates of the overall reaction of PTMOp were explained by the 'Ping-Pong' mechanism with L-Phe and L-Tyr as substrate, and by the 'sequential' mechanism with L-Trp and L-Met as substrate as described in the RESULTS section. But as reported for PAO (*24*), the steady-state kinetic data for all substrates used, such as L-Phe, β-2-thienylalanine, L-Tyr and L-Met, were explained by the 'Ping-Pong' mechanism.

Considering the similarity of the kinetic properties of PTMOp with those of PAO in the case of L-Phe, we assumed the following mechanism of reaction to explain the steady-state kinetic data for L-Phe, L-Tyr, L-Trp and L-Met as substrate (S),

$$E_{ox} + S \underset{k_{-1}}{\overset{k_{+1}}{\rightleftarrows}} E_{ox} \cdot S \underset{k_{-2}}{\overset{k_{+2}}{\rightleftarrows}} X \rightarrow E_{red} + P$$

$$X + O_2 \underset{k_{-3}}{\overset{k_{+3}}{\rightleftarrows}} X \cdot O_2 \overset{k_{+4}}{\rightarrow} E_{ox} + Q$$

where $E_{ox}$, X and $E_{red}$ represent the oxidized form of enzyme, the reduced form enzyme–imino acid complex and the reduced form of enzyme, respectively. In this scheme, the step, $X \rightarrow E_{red}$, is slower than the other steps, so the step is not considered to be involved in the overall reaction. We assumed the purple intermediate during the reduction of enzyme with L-Tyr, L-Trp and L-Met, though we did not observe its presence in the present experiments. Moreover, we did not observe directly the oxidation of X to $E_{ox}$, so we assumed a complex $X–O_2$ in the scheme. From the scheme, a reciprocal of the rate of overall reaction per enzyme unit concentration ($v/e_o$) can be expressed as:

$$\frac{e_o}{v} = \frac{k_{+2}+k_{+4}}{k_{+2}k_{+4}} + \frac{k_{-1}+k_{+2}}{k_{+1}k_{+2}[S]} + \frac{(k_{+2}+k_{-2})(k_{-3}+k_{+4})}{k_{+2}k_{+3}k_{+4}[O_2]} + \frac{k_{-1}k_{-2}(k_{-3}+k_{+4})}{k_{+1}k_{+2}k_{+3}k_{+4}[S][O_2]} \quad (1)$$

The presence of the fourth term in the equation explains that the families of lines intersect to the left of the ordinate as shown in Fig. 3B for L-Met, which indicates a sequential mechanism of catalysis. On the other hand, when X is formed irreversibly ($k_{-2} = 0$), the fourth term becomes zero in Eq. 1. Thus we get the following equation:

$$\frac{e_o}{v} = \frac{k_{+2}+k_{+4}}{k_{+2}k_{+4}} + \frac{k_{-1}+k_{+2}}{k_{+1}k_{+2}[S]} + \frac{k_{-3}+k_{+4}}{k_{+3}k_{+4}[O_2]} \quad (2)$$

This equation explains the reciprocal plots for L-Phe (Fig. 3A), which indicates a Ping-Pong type of catalysis. This is the catalytic mechanism proposed for PAO (*24*).

The maximum velocity ($V_m/e_o$) at infinite concentrations of L-amino acids and oxygen can be expressed from Eqs 1 and 2 by the following equation:

$$\frac{V_m}{e_o} = \frac{k_{+2}k_{+4}}{k_{+2}+k_{+4}}$$

This means that the maximum velocity obtained from the $e_o/v$ versus 1/[S] plot at an infinite concentration of oxygen (column 2 in Table 2) should agree with that obtained from the $e_o/v$ versus $1/[O_2]$ plot at an infinite concentration of L-amino acid (column 4 in Table 2). The values in Table 2 show that the maximum velocities obtained from the different plots agree fairly well, thus supporting the mechanism proposed. The prominent point in the kinetic parameters is that the values for the oxygenase substrate (L-Phe, L-Tyr) were higher than those of oxidase substrate (L-Met, L-Trp).

A putative Trp monooxygenase is concluded to belong to L-Phe oxidase (deaminating and decarboxylating) in the mechanism of activation, the stoichiometry of the reaction catalysed, the substrate specificity and the optimum pH. Though the catalytic mechanism proposed above for L-Phe and L-Tyr as substrate agrees well with that proposed for PAO (*24*), the spectral property of PTMOp for L-Tyr was different from that of PAO. The mechanism and its spectral property were different from that of the native PAO when L-Met was used as substrate. These might be derived from differences in the active site between these enzymes. This will be clarified by comparative studies of these enzymes from structural and mechanistic aspects.

ACKNOWLEDGEMENTS

Authors are indebted to Dr Boucher C. INRA-CNRS, France, for the kind gift of *E. coli* clone harbouring plasmid pBR322, and to Prof. Nishina Y., Faculty of Med. and Pharm. Sci., Kumamoto University, for critical reading of the manuscript.

CONFLICT OF INTEREST

None declared.

REFERENCES

1. Koyama, H. (1982) Purification and characterization of a novel L-phenylalanine oxidase (deaminating and decarboxylating) from *Pseudomonas* sp. P-501. *J. Biochem.* **92**, 1235–1240
2. Koyama, H. (1983) Further characterization of a novel L-phenylalanine oxidase (deaminating and decarboxylating) from *Pseudomonas* sp. P-501. *J. Biochem.* **93**, 1313–1319
3. Koyama, H. (1984) Oxidation and oxygenation of L-amino acids catalysed by a novel L-phenylalanine oxidase(deaminating and decarboxylating) from *Pseudomonas* sp. P-501. *J. Biochem.* **96**, 421–427
4. Koyama, H. (1984) A simple and rapid enzymatic determination of L-phenylalanine with a novel L-phenylalanine oxidase (deaminating and decarboxylating) from *Pseudomonas* sp. P-501. *Clin. Chim. Acta* **136**, 131–136
5. Nakajima, H., Koyama, H., and Suzuki, H. (1991) Immobilization of *Pseudomonas* L-Phe oxidase on a nylon membrane for possible use as an amino acid sensor. *Agric. Biol. Chem.* **55**, 3117–3118
6. Mukouyama, E. B., Suzuki, H., and Koyama, H. (1994) New subunit in L-phenylalanine oxidase from *Pseudomonas sp*. P-501 and the primary structure. *Arch. Biochem. Biophys.* **308**, 400–406
7. Suzuki, H., Higashi, Y., Asano, M., Suguro, M., Kigawa, M., Maeda, M., Katayama, S., Mukouyama, EB., and Uchiyama, K. (2004) Sequencing and expression of the L-phenylalanine oxidase gene from *Pseudomonas* sp. P-501. Proteolytic activation of the proenzyme. *J. Biochem.* **136**, 617–627
8. Salanoubat, M., Genin, S., Artiguenave, F., Gouzy, J., Mangenot, S., Arlat, M., Billault, A., Brottier, P., Camus, J.C., Cattolico, L., Chandler, M., Choisne, N.,

Claudel-Renard, C., Cunnac, S., Demange, N., Gaspin, C., Lavie, M., Moisan, A., Robert, C., Saurin, W., Schiex, T., Siguier, P., Thebault, P., Whalen, M., Wincker, P., Levy, M., Weissenbach, J., and Boucher, C.A. (2002) Genome sequence of the plant pathogen *Ralstonia solanacearum*. *Nature* **415**, 497–502

9. Altschul, Stephen F., Madden, T.L., Schaffer, A.A., Zhang, J., Zhang, Z., Miller, W., and Lipman, D.J. (1997) Gapped BLAST and PSI-BLAST: a new generation of protein data base search programs. *Nucleic Acids Res.* **25**, 3389–3402
10. Gabriel, D. W., Allen, C., Schell, M., Denny, T. P., Greenberg, J. T., Duan, Y. P., Flores-Cruz, Z., Huang, Q., M. Clifford, J., Presting, G., González, E.T., Reddy, J., Elphinstone, J., Swanson, J., Yao, J., Mulholland, V., Liu, L., Farmerie, W., Patnaikuni, M., Balogh, B., Norman, D., Alvarez, A., Castillo, J. A., Jones, J., Saddler, G., Walunas, T., Zhukov, A., and Mikhailova, N. (2006) Identification of open reading frames unique to a select agent: *Ralstonia solanacearum* Race 3 Biovar 2. *Mol. Plant-Microbe Interactions* **19**, 69–79
11. Genin, S. and Boucher, C. (2002) *Ralstonia solanacerum*: secrets of a major pathogen unveiled by analysis of its genome. *Mol. Plant Pathol.* **3**, 111–118
12. Comai, L. and Kosuge, T. (1980) Involvement of plasmid deoxyribonucleic acid in indoleacetic acid synthesis in *Pseudomonas savastanoi*. *J. Bacteriol.* **143**, 950–957
13. Hutcheson, S.W. and Kosuge, T. (1985) Regulation of 3-indoleacetic acid production in *Pseudomonas syringae* pv. *savastanoi*. Purification and properties of tryptophan 2-monooxygenase. *J. Biol. Chem.* **260**, 6281–6287
14. Spaepen, S., Vanderleyden, J., and Remans, R. (2007) Indole-3-acetic acid in microbial and microorganism-plant signaling. *FEMS Microbiol. Rev.* **31**, 425–448
15. Emanuele, J. and Fitzpatrick, P.F. (1995) Mechanistic studies of the flavoprotein tryptophan 2-monooxygenase. 1. Kinetic mechanism. *Biochemistry* **34**, 3710–3715
16. Gadda, G., Dangott, L. J., Johnson, W. H. Jr., Whitman, C. P., and Fitzpatrick, P. F. (1999) Characterization of 2-oxo-3-pentynoate as an active-site directed inactivator of flavoprotein oxidases: identification of active-site peptides in tryptophan 2-monooxygenase. *Biochemistry* **38**, 5822–5828
17. Sobrado, P. and Fitzpatrick, P. F. (2003) Analysis of the role of the active site residue Arg98 in the flavoprotein tryptophan 2-monooxygenase, a member of the L-amino oxidase family. *Biochemistry* **42**, 13826–13832
18. Ida, K., Kurabayashi, M., Suguro, M., Hiruma, Y., Hikima, T., Yamomoto, M., and Suzuki, H. (2008) Structural basis of proteolytic activation of L-phenylalanine oxidase from *Pseudomonas* sp. P-501. *J. Biol. Chem.* **283**, 16584–16590
19. Moore, J.T., Uppal, A., Maley, F., and Maley, G.F. (1993) Overcoming inclusion body formation in a high-level expression system. *Protein Express. Purif.* **4**, 160–163
20. Cornish-Bowden, A. (1976) *Estimation of rate constants in* Principles of Enzyme Kinetics.pp. 168–193, Butterworths, London-Boston
21. Kawamura-Konishi, Y., Asano, A., Yamazaki, M., Tashiro, H., and Suzuki, H. (1998) Peroxidase activity of an antibody-ferric porphyrin complex. *J. Mol. Catalysis. B: Enzymatic.* **4**, 181–190
22. Kawamura-Konishi, Y., Tsuji, M., Hatana, S., Asanuma, M., Kakuta, D., Kawano, T., Mukouyama, E. B., Goto, H., and Suzuki, H. (2007) Purification, characterization, and molecular cloning of tyrosinase from *Pholiota nameko*. *Biosci. Biotechnol., Biochem.* **71**, 1752–1760
23. Combet, C., Jambon, M., Deleage, G., and Geourjon, C. (2002) Geno3D: automatic comparative molecular modeling of protein. *Bioinformatics* **18**, 213–214
24. Koyama, H. and Suzuki, H. (1986) Spectral and kinetic studies on *Pseudomonas* L-phenylalanine oxidase (deaminating and decarboxylating). *J. Biochem.* **100**, 859–866